X-ray photoemission, bremsstrahlung isochromat, Auger-electron, and optical spectroscopy studies of Y-Ba-Cu-O thin films

D. van der Marel
Faculty of Applied Physics, Delft University of Technology, Lorentzweg 1, 2628 CJ Delft, The Netherlands

J. van Elp and G. A. Sawatzky
Faculty of Applied Physics, Groningen University, Nijenborgh 18, 9747 AG Groningen, The Netherlands

D. Heitmann
Max-Planck Institut für Festkörperphysik, Heisenbergstrasse 1, 7000 Stuttgart 80, Federal Republic of Germany
(Received 21 October 1987; revised manuscript received 19 January 1988)

We have investigated the electronic structure of $YBa_2Cu_3O_7$ thin films using a variety of spectroscopic methods. From a comparison of the copper and oxygen Auger spectra with the valence-band spectra we conclude that the on-site repulsion U between the valence electrons is fairly high both on copper and oxygen sites. A strong satellite is found in the copper $2p$ spectra, indicating a d^9 configuration of most copper atoms. The shape of the oxygen $1s$ line is found to depend strongly on the oxygen concentration. In both the occupied and unoccupied states as measured by x-ray photoemission spectroscopy and bremsstrahlung isochromat spectroscopy the density close to the Fermi level is very low and the consequences hereof are discussed. From the room-temperature optical spectra we find evidence for metallic behavior and a longitudinal mode at about 0.8 eV which we interpret as a plasmon.

INTRODUCTION

Numerous theoretical models have been proposed as possible explanations for the high-T_c (Refs. 1 and 2) behavior. These range from the more conventional band-structure calculations involving very large electron-phonon interactions and nesting characteristics to model Hamiltonians based on the assumption of large electron-electron interactions on the Cu sites in which the dominant role has been played by the Hubbard Hamiltonian, which is a single-band approach.[3-6] A better choice for the high-T_c superconductors is a two-band model involving the almost degenerate O $2p$ and Cu $3d$ states, as has been emphasized by several authors.[7-9]

Recently Zaanen, Sawatzky, and Allen (ZSA) proposed a two-parameter classification scheme for the transition-metal compounds[10,11] characterized by the parameters U/T and Δ/T. U is the electron-electron interaction at the transition-metal site, Δ is the energy involved in transferring an electron from the ligand band to an empty transition-metal d state, and T is the p-d transfer-matrix element. If $\Delta > U$ the lowest-lying electron-hole excitations are d-d interatomic hops and a Mott-Hubbard-type metal-insulator transition takes place as function of U/T (region A of the ZSA scheme). In the opposite case, $\Delta < U$, the lowest-lying excitations are of the charge-transfer type (region B of the ZSA scheme) and the system is a so-called charge-transfer semiconductor for sufficiently large Δ/T. As we will see below, this is also the more relevant region for the high-T_c superconductors.

The stoichiometric compounds La_2CuO_4 and $YBa_2Cu_3O_{6.5}$ would then be semiconductors with a gap of charge-transfer type. Important here is that the first ionization states in phase B are of primarily O $2p$ character with some admixture of Cu^{3+} (d^8) character. Upon substitution (replacement of La by Ba, Sr, or the addition of oxygen) the charge is then compensated by "holes" of primarily O $2p$ character. This would lead to a basic starting point different from that suggested by the Hubbard Hamiltonian which involves states of primarily Cu $3d$ character, i.e., region A in the ZSA scheme. It is, of course, of utmost importance to establish which of the three starting points just mentioned are closest to the actual electronic structure of the high-T_c materials. In terms of the ZSA scheme we would like to then have estimates of the magnitudes of the bandwidths, covalent interactions, and hybridization interactions.

In this paper we present some results obtained from experiments done on thin films of the $YBa_2Cu_3O_{7-y}$ samples. In the various forms of spectroscopy [optical, electron energy loss, (inverse) photoelectron spectroscopy, and Auger spectroscopy] the rough surfaces of sintered ceramic samples can and have caused inferior signal-to-noise ratios resulting in long measuring times. The thin-film samples used are optically flat and at least our experience is that the count rate in for example x-ray photoemission spectroscopy (XPS) is at least an order of magnitude larger. Also, there is no influence of diffuse scattering in the optical reflectivity data at short wavelengths.

SAMPLE PREPARATION AND CHARACTERIZATION

We report on XPS, Auger electron spectroscopy, bremsstrahlung, isochromat spectroscopy (BIS), and optical reflection experiments on thin films of YBaCuO that showed a resistive transition starting at approximately 90 K and ending at about 45 K. The samples were prepared

by means of metal evaporation from three different sources (two *e*-beam, one effusion cell) while simultaneously directing a beam of oxygen at the samples[12] followed by subsequent heating in an oxygen atmosphere during several hours at a temperature of 1150 K. We used single-crystal Al_2O_3 substrates. The samples are shiny and black. The composition as determined from microprobe analysis is within 3% of the nominal 1:2:3:7 composition range. The x-ray diffraction patterns revealed that the samples consist of polycrystalline $YBa_2Cu_3O_{7-y}$ and some additional phases. Due to a large linewidth, the orthorhombic splitting in the diffraction pattern was not well resolved. From scanning electron microscopy studies and inspection with an optical microscope we know that the samples consist of areas of approximately 20 μm^2 separated by narrow veins of a different composition. From scanning Auger analysis we estimated that less than 1% of the surface is formed by the nonsuperconducting viens, so that this part of the films has negligible influence on the experiments discussed in this paper. The influence on the in-plane resistivity is, however, very strong due to a two-dimensional percolation-type conductivity limited by the nonsuperconducting vein structure. This explains the relatively wide resistive transition, even though the samples are almost stochiometric. For a detailed discussion on the preparation and characterization of the thin films studied in this paper we refer to Ref. 12.

CORE-LEVEL SPECTRA

The sample was inserted into the XPS chamber 4 weeks after preparation. The bulk of the samples still showed superconducting properties. Although it was kept in a clean environment, the XPS wide scans taken immediately after insertion showed a strong carbon 1*s* doublet at 289 and 284.5 eV binding energy. Clear peaks of Cu, Ba, Y, and O were also visible. No other elements could be detected. The Cu 2*p* line had a weak satellite at the high binding-energy side. As the surface was clearly contaminated, we tried the following cleaning procedure: First we cleaned the surface with Ar bombardment using 2 keV Ar^+ ions. Then we baked the sample during 30 min at a temperature of 640 K under oxygen at a pressure of 0.01 Torr. After a few cycles we obtained a clean surface (less then 0.3 carbon atom per formula unit) while the composition as determined from the XPS peak intensities[13] was close to stoichiometry. We took XPS spectra after each step in order to monitor the changes in composition and to see, whether there were chemical shifts or changes in line shape.

Immediately after Ar-ion etching, the apparent oxygen concentration was always too high: typically we found 1:2:2.5:8.2. This extra intensity of the oxygen line was mainly contained in a shoulder on the high binding-energy side of the O 1*s* peak. After baking in oxygen the intensity of the O 1*s* peak has decreased (composition 1:1.6:2.2:5.9), except in cases where also a strong carbon signal was found. Apparently, contamination with carbon monoxide had occurred in the latter cases. After a few cycles of etching and heating in oxygen these contaminants

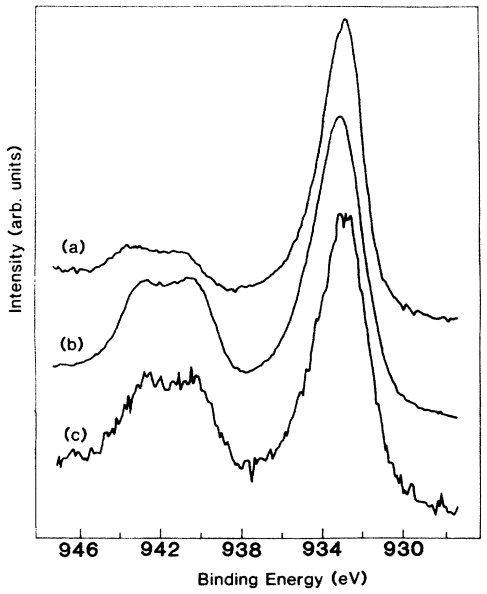

FIG. 1. XPS spectra of the Cu $2p^{3/2}$ lines. Curve (a): after Ar-ion etching. Curve (b): after annealing in oxygen. Curve (c): after electron-gun operation.

disappeared. Just after Ar etching the Cu 2*p* satellite weakened considerably. After baking in oxygen the total intensity of this satellite was about 54% of the main-line intensity. In Figs. 1 and 2 we show the Cu $2p^{3/2}$ and the O 1*s* lines after different surface treatments. The Cu 2*p* data of the samples after baking are in good agreement with results obtained on sintered samples.[14–17]

In the BIS experiments which we will describe below, electrons were emitted from a BaO cathode a few cm

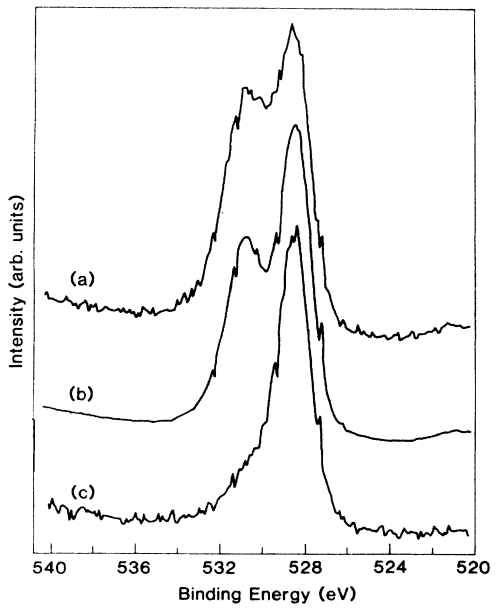

FIG. 2. XPS spectra of the O 1*s* line. Curve (a): after Ar-ion etching; curve (b): after annealing in oxygen; curve (c): after electron-gun operation.

away from the sample surface. XPS spectra taken after extensive electron gun operation revealed a further decrease in the oxygen 1*s* intensity. The shoulder at the high binding-energy side of the peak had vanished almost completely, while the intensity of the main line had increased. The shape and relative intensity of the Cu 2*p* main line and satellite were not affected.

We interpret these observations as follows: After Ar-ion etching the sample surface is probably amorphous. Most Cu atoms are in 1^+ state and do not show satellite behavior. There is an excess of oxygen atoms which are in a low ionization state, which could indicate the formation of peroxide bonds. The heat treatment restores stoichiometry, resulting in Cu atoms in the 2^+ state. The XPS spectra of the 2*p* line are now very similar to the spectra of copper monoxide and the copper dihalides:[18] The satellite peak corresponds to the unscreened $\underline{2p}3d^9$ state. The main line corresponds to the screened $\underline{2p}3d^{10}\underline{L}$ final states, where a ligand electron is pulled in the empty *d* state. The spread in intensity of the satellite over approximately 5 eV results from multiplet splitting of the $\underline{2p}3d^9$ final states. The shoulder at the high binding-energy side of the oxygen 1*s* peak indicates the presence of two types of oxygen, either due to sites with different Madelung potentials or due to different ionization states of the O atoms. Electron-gun operation apparently removes some of the oxygen that causes the high binding-energy shoulder of the 1*s* peak, probably due to heating. Since the Cu 2*p* line shape has not changed, it is unlikely that the removal of some of the oxygen influences the electronic configuration of the Cu atoms.

VALENCE-BAND SPECTRA

In Fig. 3 we display the XPS spectrum taken with Al $K\alpha$ radiation and the BIS spectrum with a monochromator window at 1486.6 eV. The structure at about 14–15 eV binding energy is due to the Ba 5*p* spin-orbit split doublet. The shoulder at about 10 eV binding energy is usually attributed to a "satellite" which in this case would have predominantly Cu d^8 final-state character. The broad structure between 0 and about 7 eV is then assigned to predominantly O 2*p* states or, in configuration interaction language, $3d^9\underline{L}$ final states where $\underline{L}$ designates a ligand (O 2*p*) hole. As observed in numerous other investigations the density of states observed close to the Fermi level is very small and is more typical of a semiconducting rather then a metallic system. From band-structure calculations[19] one would expect a sizable density of states at E_F. This discrepancy is due to the strong electron-electron correlations. Usually, if strong correlations are present, band-structure calculations based on the local density approach do not provide the correct single hole or single electron excitation energies. In Fig. 3 we also display the BIS spectrum of the conduction bands taken with incident electrons having a kinetic energy of about 1500 eV and using a monochromator with a window at 1486.6 eV for bremsstrahlung detection. We interpret the peak at 2.5 eV as the Cu d^{10} final state. The wide band starting at about 8 eV then consists of mixed O 3*s*, Cu 4*s*, Ba 5*d*, and Y 4*d* character, while the narrow peak at 15 eV is formed by the unoccupied Ba 4*f* resonance. The total resolution of the BIS setup is about 0.7 eV, so that the tail extending to the Fermi energy is probably due to instrumental broadening. We have to add that, as we mentioned before, the oxygen concentration is influenced by electron-gun operation, so that this spectrum corresponds to a sample with a relatively low oxygen concentration. We do not expect this to influence the nature of the Cu d^{10} final state, as we have already seen, that the copper core-level spectra remain unaffected by the oxygen deficiency. Our measurements do not rule out the possibility of O 2*p* character near E_F, as for Al $K\alpha$ radiation the O 2*p* photoelectron cross section is very small relative to the Cu 3*d* cross section.[13] This means that the XPS and BIS spectra effectively reflect the density of states at the copper sites. High-energy electron-energy-loss studies of the O 1*s* to O 2*p* threshold indicate a sizable amount of oxygen 2*p* character at the Fermi level.[20]

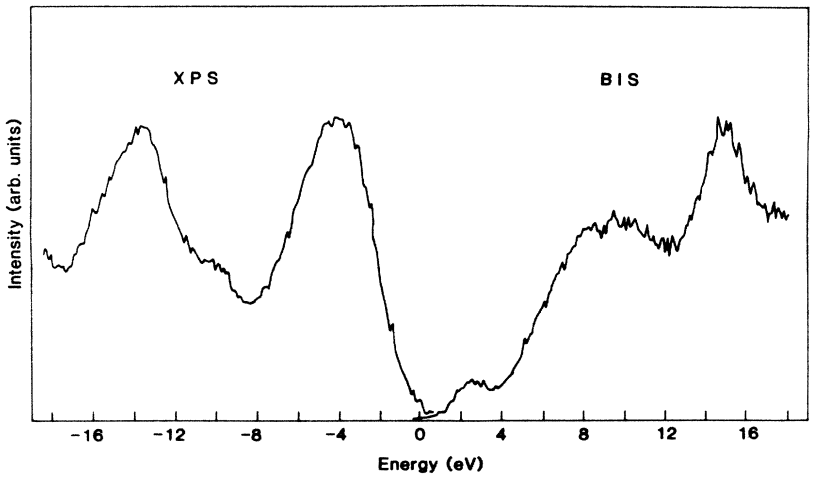

FIG. 3. XPS and BIS valence-band spectra of $Y_1Ba_2Cu_3O_7$.

AUGER SPECTRA

We measured the Cu $L_3M_{4,5}M_{4,5}$ Auger spectra and the O $K_1L_{2,3}L_{2,3}$ Auger spectra in order to determine the value of the valence hole-hole interaction energies at the Cu and the O sites. These spectra are displayed in Figs. 4 and 5. We used the Al $K\alpha$ x-ray source for excitation. The initial state of the Cu *LMM* Auger spectra is formed by the final state of the $2p$ core-level excitation. From the discussion of Fig. 1 we know that this final state splits in two sets of eigenstates due to the presence of the core hole: The d^9 states and the $d^{10}\underline{L}$ states. These form the initial states of the Auger process, so that the final states of the *LMM* Auger process are formed by the d^7 and the $d^8\underline{L}$ multiplets. The kinetic energy of the Auger electron is given by $E=E_c-E(h,h)$, i.e., the core-hole binding energy minus the energy of two holes located at the same copper site. To get an idea of the value of the two-hole energies we also indicated the threshold energy corresponding to the fully screened initial states. If we compare these spectra to those of metallic copper[21,22] we see two main differences: (1) The features in our spectra are less sharp and (2) there is extra intensity at kinetic energies of about 914 eV. Both features have been discussed for the Cu halides by van der Laan, Westra, Haas, and Sawatzky,[18] who attribute the smoothing of the spectrum to crystal-field splitting resulting in a splitting of the ^1G, ^3P, ^1D, and ^3F final states. Another source of broadening is formed by the finite lifetime due to coupling of the d^8 states to the $d^9\underline{L}$ continuum. van der Laan attributes the extra intensity at the left side of the ^1G line to the d^7 final states originating from the unscreened $\underline{2p}3d^9$ state. These extra lines coincide almost completely with the positions of the Auger transitions preceded by the $L_2L_3M_{4,5}$ Koster-Kronig process [22] which also end up as $3d^7$-like states. (Through this process the $L_3M_{4,5}M_{4,5}$ line "borrows" intensity from the $L_2M_{4,5}M_{4,5}$ line.)

In Fig. 5 we display the oxygen *KLL* Auger spectrum. The $1s$ threshold is located at 528 eV. The peak of the *KLL* spectrum corresponds to approximately 15 eV binding energy of the hole pair. From Fig. 3 we estimate that the center of the valence band lies at about 5 eV binding energy. Assuming that this is also the average O $2p$ binding energy, we arrive at an effective U of about 5 eV for the oxygen $2p$ holes. Such high values of the oxygen $2p$ Coulomb interactions have also been observed in other transition-metal oxides.[23] This is about as large as the bandwidth, which is also of the order of 5 eV. So we see that also the oxygen $2p$ bands must be considered as bands of strongly interacting particles. In the limit of fully occupied $2p$ bands this has no physical consequences. If we start emptying these bands, however, as is the case in the high-T_c superconductors, correlation effects become important.

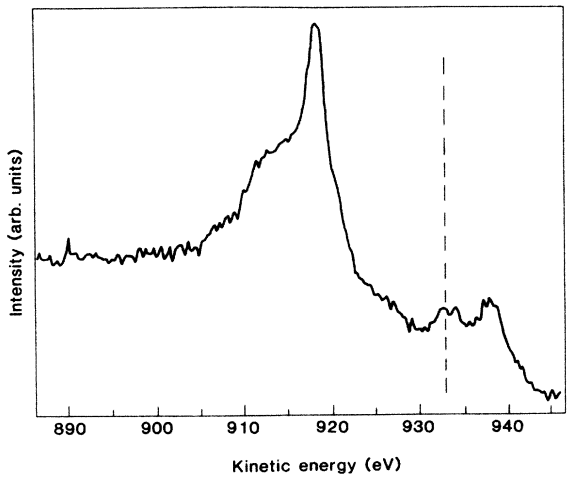

FIG. 4. Cu *LMM* Auger spectrum taken after annealing in oxygen.

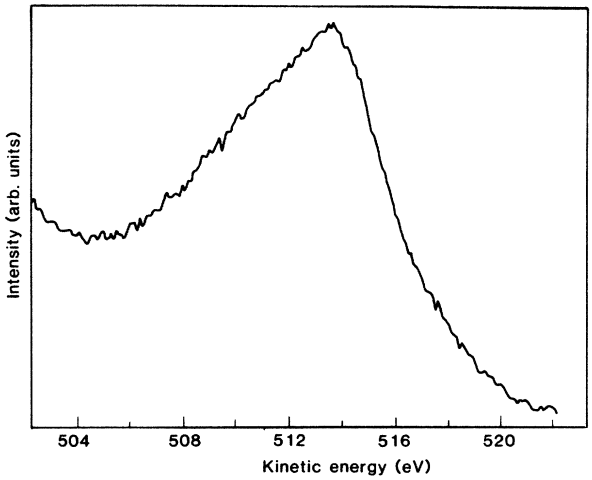

FIG. 5. O *KLL* Auger spectrum taken after annealing in oxygen.

OPTICAL SPECTRA

We collected optical reflectance spectra in the energy range between 0.1 and 6 eV at room temperature. In Fig. 6 we present the results. The dielectric function was determined from the spectra by means of Kramers-Kronig analysis. We approximated the part above 6 eV by a Lorentzian peak in the dielectric function centered around 10 eV with a full width at half maximum (FWHM) of 4 eV. Its height was used as a free parameter while fitting the Kramers-Kronig consistent dielectric function to the reflectivity data. At energies below 0.1 eV the reflectivity is about 80% in the whole wavelength range, except where phonon structure of (below 90 K) superconducting gap structure occurs. The data between 0.3 and 0.5 eV are uncertain, as we had to add two spectra from different spectrometers. The spectra had overlap in an energy range where the instrumental accuracy of both instruments was rather low. In Fig. 7 we display the resulting dielectric function.

The real part of the dielectric function crosses zero at about 0.8 eV. We interpret the corresponding longitudinal mode as the plasmon mode. Extrapolation of the resitivity function to zero energy gives a resistivity of about 1000 $\mu\Omega$ cm. Typical values from room-temperature four-terminal resistance measurements of our samples are 10000 $\mu\Omega$ cm. As mentioned in the Introduction, the

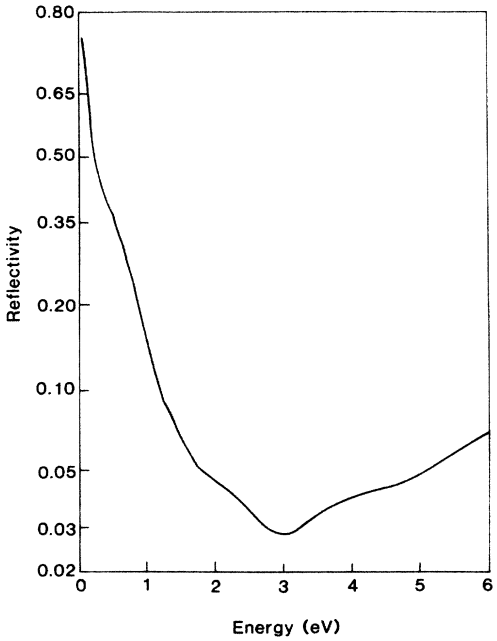

FIG. 6. Experimental reflectivity spectrum.

latter method gives a higher resistance due to barriers formed in inhomogeneities. If we assume, that a simple Drude model can be used at low energies, we can use the Drude formula for the resistivity together with our zero energy value for ρ and 0.8 eV for the plasmon energy to estimate τ which amounts to approximately 4×10^{-15} sec. If we use the free-electron mass and the Drude formula for the plasmon energy we find a carrier density of 7.3×10^{20} cm^{-3}. This corresponds to 0.12 elementary charge per unit cell, which is a factor of 9 lower than expected if every excess oxygen atom contributes two charge carriers. This suggests a carrier effective mass of about nine times the free-electron value. We have the feeling, however, that a more careful analysis is required, which takes into account the anisotropic nature of the electronic structure, together with a proper description of the excitonic contributions to the dielectric function.

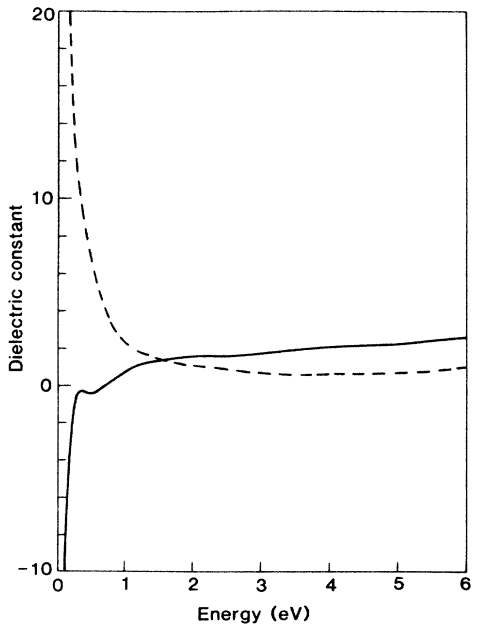

FIG. 7. Dielectric function obtained from Kramers-Kronig analysis. Solid curve: real part; dashed curve: imaginary part.

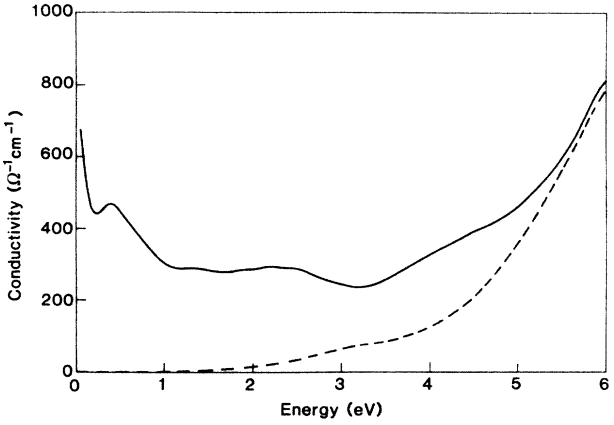

FIG. 8. Conductivity function obtained from Kramers-Kronig analysis (solid curve) and convolution of the BIS and XPS spectra of Fig. 3 (dashed curve).

In Fig. 8 we display the optical conductivity, which was calculated from the imaginary part of the dielectric function of Fig. 7. There are broad structures in the conductivity plot near 1.3 and 2.3 eV, followed by a minimum at 3.2 eV and a wide absorption band at higher energies with some structure around 3.3 eV. There is some additional structure at 0.4 eV, which coincides with the peak observed by Kamaras *et al.*[24] and which has been interpreted as a charge-transfer exciton.[25] To point out where our combined BIS and XPS results put the onset of interband transitions, we also plot the convolution of the spectra of Fig. 3, which corresponds to the experimentally determined joint density of states, apart from optical matrix elements and selection rules. We see that the main increase starts around 3 eV so that the structure at 1.3 and 2.3 eV cannot be due to straightforward interband transitions. We speculate that these structures are pulled out of the continuum of interband transitions due to electron-hole interactions. They could be either of the charge transfer type involving an electron at a copper site and a hole at a neighboring oxygen site, or forbidden transitions within the Cu *d* shell. Recent band-structure calculations[26] also predict a broad structure at about 2 eV. As these authors did not take into account the strong electron-electron interactions this coincidence may seem a bit surprising. However, these interactions are at least partly compensated in an exciton due to the fact that local charge neutrality is maintained.

CONCLUSIONS AND DISCUSSION

The above described experimental results show that the local electronic structure of Cu is similar to that of Cu in

$CuCl_2$, $CuBr_2$, or CuO.[18] This follows both from the similarity of the Cu $2p$ satellite, energy and intensity as well as the $L_{2,3}M_{4,5}M_{4,5}$ Auger line shape. This leads us to the conclusion, that $U(dd)$ is about 5 to 7 eV, which places these materials in the strongly correlated class. In addition, again by comparison to the $CuCl_2$ case, we also are led to conclude that the charge-transfer energy $\Delta = E(d^9\underline{L}) - E(d^{10})$ is 1–2 eV or considerably less than $U(dd)$. This puts these materials in class B of the ZSA phase diagram. Important then is that upon addition of oxygen to the "stoichiometric" $YBa_2Cu_3O_{6.5}$ the holes required for charge neutrality will be of primarily O $2p$ character rather than Cu $3d$ character. The metallic character therefore is due to holes in the oxygen p band although hybridization will always mix in some $Cu(d^8)$ character. In view of this the finding, that the oxygen $2p$ intraatomic Coulomb interaction $[U(pp) = 5$ eV] is also large, is highly significant.

From our analysis of the optical data we find metallic behavior at low frequencies. The real part of the dielectric function crosses zero at 0.8 eV, which we interpret as the plasmon frequency. At lower frequencies the dielectric constant shows divergent behavior typical for metallic systems. There are several broad structures in the conductivity plot between 1 and 3 eV which we interpret as transitions of excitonic origin.

ACKNOWLEDGMENTS

We would like to thank A. Breitochwerdt for his assistance with the ir measurements and Professor J. C. Fuggle for a critical reading of the manuscript. This work is supported by the Stichting voor Fundamenteel Onderzoek der Materie and was made possible by financial support from the Nederlandse Organisatie voor Zuiver Wetenschappelijk Onderzoek.

[1] J. G. Bednorz and K. A. Müller, Z. Phys. B **64**, 188 (1986).
[2] C. W. Chu, P. H. Hor, R. L. Meng, L. Gao, Z. J. Huang, and Y. Q. Wang, Phys. Rev. Lett. **58**, 405 (1987).
[3] P. W. Anderson, Science **235**, 1196 (1987).
[4] S. A. Kivelson, D. S. Rokhsar, and J. P. Sethna, Phys. Rev. B **35**, 8865 (1987).
[5] W. Metzner and E. Vollhardt, Phys. Rev. Lett. **59**, 121 (1987).
[6] C. Gros, R. Joynt, and T. M. Rice, Z. Phys. B **68**, 425 (1987).
[7] V. J. Emery, Phys. Rev. Lett. **58**, 2794 (1987).
[8] J. E. Hirsch, Phys. Rev. Lett. **59**, 228 (1987).
[9] Z. Shen, J. W. Allen, J. J. Yeh, J. S. Kang, W. Ellis, W. Spicer, I. Lindau, M. B. Maple, Y. Dalichaouch, M. S. Torikachvili, J. Z. Sun, and T. H. Geballe, Phys. Rev. B **36**, 8414 (1987).
[10] J. Zaanen, G. A. Sawatzky, and J. W. Allen, Phys. Rev. Lett. **55**, 418 (1985).
[11] G. A. Sawatzky, and J. W. Allen, Phys. Rev. Lett. **53**, 2239 (1985).
[12] A. J. G. Schellingerhout, R. H. M. van der Leur, D. Schalkoord, D. van der Marel, and J. E. Mooij (unpublished).
[13] J. H. Scofield, J. Electron Spectrosc. Relat. Phenom. **8**, 129 (1976).
[14] A. Fujimori, E. Takayama-Muromacki, and Y. Uchida, Solid State Commun. **63**, 857 (1987).
[15] P. Steiner, V. Kinsinger, I. Sander, B. Siegwart, S. Huefner, C. Politis, R. Hoppe, and H. P. Mueller, Z. Phys. B **67**, 497 (1987).
[16] P. Steiner, V. Kinsinger, I. Sander, B. Siegwart, S. Huefner, and C. Politis, Z. Phys. B **67**, 19 (1987).
[17] P. Thiry, G. Rossi, D. W. Niles, R. Joynt, G. Maragaritondo, N. G. Stoffel, and J. M. Tarascon (unpublished).
[18] G. van der Laan, C. Westra, C. Has, and G. W. Sawatzky, Phys. Rev. B **23**, 4369 (1981).
[19] L. F. Mattheiss and D. R. Hamann, Solid State Commun. **63**, 395 (1987).
[20] N. Nucker, J. Fink, J. C. Fuggle, P. J. Durham, and W. M. Temmerman (unpublished); N. Nucker, J. Fink, B. Renker, D. Ewer, C. Politis, P. J. W. Weijs, and J. C. Fuggle, Z. Phys. B **67**, 9 (1987).
[21] E. Antonides, E. C. Janse, and G. A. Sawatzky, Phys. Rev. B **15**, 4596 (1977).
[22] H. Haak, Ph.D. thesis, Groningen University, 1983 (unpublished).
[23] G. A. Sawatzky and D. Post, Phys. Rev. B **20**, 1546, (1979).
[24] K. Kamaras, C. D. Porter, M. G. Doss, S. L. Herr, D. B. Tanner, D. A. Bonn, J. E. Greedan, A. H. O'Reilly, C. V. Stager, and T. Timusk, Phys. Rev. Lett. **59**, 919 (1987).
[25] C. M. Varma, S. Schmitt-Rink, and E. Abrahams, in *Novel Superconductivity,* Proceedings of the International Workshop on Novel Mechanisms of Superconductivity, Berkely, 1987, edited by V. Z. Kresin and S. A. Wolf (Plenum, New York, 1987).
[26] G. Zhao, Y. Xu, W. Y. Ching, and K. W. Wong, Phys. Rev. B **36**, 7203 (1987).